Moreno, P.; López Del Rincón, C.; Ruiz-Ruiz, S.; Peña Garcia, L.; Guerri, J. (2022). From the smallest to the largest subcellular plant pathogen: Citrus tristeza virus and its unique p23 protein. Virus Research. 314(198755):1-13. https://doi.org/10.1016/j.virusres.2022.198755

Review article

From the smallest to the largest subcellular plant pathogen: Citrus tristeza virus and its unique p23 protein

Pedro Moreno [a, 1], Carmelo López [b], Susana Ruiz-Ruiz [c], Leandro Peña [d], José Guerri [a]

[a] Instituto Valenciano de Investigaciones Agrarias (IVIA), Moncada, 46113-Valencia, Spain. (Retired)
[b] Instituto de Conservación y Mejora de la Agrodiversidad Valenciana (COMAV), Universitat Politècnica de València, 46022-Valencia, Spain.
[c] Unidad Mixta de Investigación en Genómica y Salud, Fundación para el Fomento de la Investigación Sanitaria y Biomédica de la Comunitat Valenciana (FISABIO). 46022-Valencia, Spain.
[d] Instituto de Biología Molecular y Celular de Plantas (IBMCP). Consejo Superior de Investigaciones Científicas (CSIC)-Universidad Politécnica de Valencia (UPV). 46022-Valencia, Spain.

[1] Corresponding author:
E-mail address: pedromoreno.ivia@gmail.com
Present address: C/Bilbao 49, Apt. 19, 46009-Valencia, Spain.

From the smallest to the largest subcellular plant pathogen: Citrus tristeza virus and its unique p23 protein

Abstract

Knowledge on diseases caused by *Citrus tristeza virus* (CTV) has greatly increased in last decades after their etiology was demonstrated in the past seventies. Professor Ricardo Flores substantially contributed to these advances in topics like: i) improvement of virus purification to obtain biologically active virions, ii) sequencing mild CTV isolates for genetic comparisons with sequences of moderate or severe isolates and genetic engineering, iii) analysis of genetic variation of both CTV genomic RNA ends and features of the highly variable 5' end that allow accommodating this variation within a conserved secondary structure, iv) studies on the structure, subcellular localization and biological functions of the CTV-unique p23 protein, and v) potential use of *p23* and other 3'-proximal regions of the CTV genome to develop transgenic citrus resistant to the virus. Here we review his main achievements on these topics and how they contributed to deeper understanding of CTV biology and to new potential measures for disease control.

Keywords: CTV pathogenicity, CTV resistance, p23 protein, subcellular localization, virus-host interaction, p23-transgenic citrus

1. Introduction

Ricardo Flores, former research professor of the *Instituto de Biología Molecular y Celular de Plants* (IBMCP, Valencia, Spain), is best known among plant virologists for his important contributions on viroid identification and studies on their molecular biology, RNA conformation and replication, genetic variability and pathogenicity mechanisms. However, his scientific interest, starting with his Ph.D. studies and later continued up to his last days, also included *Citrus tristeza virus* (CTV), a major citrus pathogen considerably different from the viroid plant pathogens. His achievements on this subject were also outstanding and included improvements in virion purification, sequencing of new virus isolates, analysis of

variability of the 5'- and 3'-terminal regions of the viral genome, and above all, studies on biological and structural characterization of the CTV-encoded p23 protein and on its potential use to disease control.

Here we discuss the significance of these achievements in their historical context and how they contributed to future advances in understanding CTV biology and developing new disease control measures.

2. First steps to establish the etiology of the tristeza disease of citrus

Tristeza disease was first recognized in Brazil and Argentina in the 30s-40s of the past century, as a decline and death syndrome shown by most citrus varieties propagated on sour orange (SO) (*Citrus aurantium* L.) rootstock. A similar disease, called quick decline was also observed in California. Resistance of SO to the root and crown rot disease, together with its excellent agronomic characteristics, were critical for the rapid increase of the citrus industry in the first third of the twentieth century, but it also created the conditions for the disaster occurred after introduction and dispersal of CTV (Bar-Joseph et al., 1989; Moreno and Garnsey, 2010).

CTV likely appeared in southeastern China, the site of origin of many citrus species, and likely co-evolved there with citrus, its unique natural host, to cause a phloem-restricted infection, often symptomless. Citrus were later brought to other areas in the world, first using seeds that are unable to transmit the virus, but after improvements of maritime transports, budsticks and whole plants were moved to different countries and CTV with them. When the virus met a new type of host [sweet orange (SwO) (*C. sinensis* (L.) Osb.), mandarin (M) (*C. deliciosa* Blanco) or grapefruit (Gf) (*C. paradisi* Macf.) propagated on SO] that was sensitive to CTV-induced decline, the first tristeza epidemics appeared (Fig. 1A). Some countries like South Africa or Australia did not suffer these epidemics because they were unable to grow SwO propagated on SO and they used other rootstocks like rough lemon (RL) (*C. jambhiri* Lush) or trifoliate orange (TfO) (*Poncirus trifoliata* (L.) Raf.) that do not show CTV decline (Bar-Joseph et al., 1989; Moreno et al., 2008; Moreno and Garnsey, 2010). However, these countries would be seriously affected

by stem pitting (SP), another CTV-induced disease affecting mainly acid lime (Lm) (*C. aurantifolia* (Christm.) Swing), Gf and SwO varieties (Fig. 1B). A third syndrome called seedling yellows (SY) was also found in Australia, South Africa and later in other regions, which consists of leaf yellowing, stunting and finally growth cessation of SO, Gf or lemon (L) (*C. limon* (L.) Burn. f.) seedlings inoculated with certain virus isolates (Fig. 1C). This syndrome is mainly used to characterize virus isolates in the greenhouse, but it is rarely observed in the field (Moreno and Garnsey, 2010).

In California, quick decline was shown to be an infectious disease that could be graft-transmitted and naturally spread in the field (Fawcett and Wallace, 1946). This same year, in Brazil, tristeza was transmitted from infected to healthy plants by *Toxoptera citricida* (Kirkaldy) (Meneghini, 1946), indicating that this (and other) aphid species could act as natural vector. These findings and failure to detect fungi or bacteria associated with quick decline- or tristeza-affected trees suggested that a virus should be the causal agent of both diseases. Much later, Kitajima et al. (1964) observed at the electron microscope that infected, but not healthy trees, had associated filamentous particles (about 2000 nm length and 10-12 nm diameter, Fig. 1D), with helical structure and an internal channel, resembling the virions of *Beet yellows virus* (BYV).

The first purification procedure allowing to obtain enough virions for physical and chemical characterization (Bar-Joseph et al., 1972), used density gradient centrifugation in cesium chloride, after fixation with formaldehyde. Fixation was necessary because cesium chloride caused virion degradation, but at the same time, fixed particles became biologically inactive. Based on the orcinol test, purified particles were shown to contain RNA, but no DNA, and electrophoresis analysis showed a 25-kDa capsid protein.

By the time that Bar-Joseph's paper appeared, Ricardo Flores started his PhD research with the objective of improving the CTV purification procedure at the Instituto de Agroquímica y Tecnología de Alimentos (IATA) (part of the IATA laboratories would later integrate in the IBMCP). He also used differential centrifugation, but introducing a critical modification: in the gradient centrifugation

step, he used cesium sulphate instead of cesium chloride (Flores et al., 1975). This modification obviated the need for virion fixation and allowed to obtain biologically active virions, which paved the way to prove that mechanical inoculation of the purified filamentous particles by bark slash-cut in healthy citrus plants induced the symptoms characteristic of tristeza (Garnsey et al., 1977), thus proving that CTV was the causal agent of citrus tristeza or quick decline diseases.

3. Coming back to dissecting the genome and molecular biology of CTV

After getting his PhD, Ricardo moved to the Joseph Semancik's lab (University of California, Riverside) where he entered in contact with the rapidly increasing viroid world that he would never abandon in his career. However, he did not completely forget CTV, his first scientific love. Thus, when in the middle 90s he was invited by his colleagues of the Virology, Molecular Biology and Plant Transformation laboratories of the *Instituto Valenciano de Investigaciones Agrarias* (IVIA) to cooperate in an international project on CTV, he gladly accepted their invitation and continued this collaboration for the rest of his professional life.

In this 20-year span (1975-1995) knowledge on CTV and tristeza disease had greatly expanded. Similarities between CTV and BYV led to the establishment of a new taxonomic group called Closteroviruses (Bar-Joseph et al., 1979a), which later would develop to become the family *Closteroviridae* (Fuchs et al., 2020). Improved purification procedures not only enabled to proof the etiology of tristeza disease (Garnsey et al., 1977), but also to develop CTV-specific polyclonal and monoclonal antibodies (Gonsalves et al., 1978; Vela et al., 1986) for quick and sensitive detection of the virus by enzyme-linked immunosorbent assay (ELISA) (Bar-Joseph et al., 1979b; Cambra et al., 1979; Garnsey et al., 1993). In turn, availability of ELISA procedures suited for massive indexing, allowed studying CTV epidemiology under different field conditions (Gottwald et al., 1996, 1998).

4. Sequencing the genomic RNA of CTV

A major breakthrough in the CTV knowledge was obtaining the complete genomic sequence of the isolate T36 from Florida (Karasev et al., 1995; Pappu et

al., 1994), which revealed a single-stranded (ss), positive-sense genomic RNA (gRNA) of almost 20 kilobases, organized in 12 open reading frames (ORFs) and two untranslated regions (UTRs) of 107 and 273 nucleotides (nt) at the 5' and 3' ends, respectively (Fig. 1E). ORFs 1a and 1b, in the 5' half of the gRNA, encode proteins of the replicase complex, whereas ORFs 2 through 11, spanning the 3' moiety, encode proteins p33, p6, p65, p61, p27, p25, p18, p20, p13 and p23, involved in virion assembly (p65, p61, p27 and p25), movement (p33, p6, p65, p61, p27, p25 and p23), host range (p33, p18 and p13), RNA silencing (RS) suppression (p25, p20 and p23), pathogenicity (p33, p18, p13 and p23) and interaction with other viral proteins and superinfection exclusion (p33) (Albiach-Martí et al., 2010; Bak and Folimonova, 2015; Dao et al., 2020; Dawson et al., 2013; Folimonova, 2013; Ghorbel et al., 2001; Lu et al., 2004; Tatineni and Dawson 2012; Tatineni et al., 2011). Northern blot hybridization with probes complementary to the different ORFs showed that ORFs 1a and b were expressed by direct translation from the gRNA, eventually using a +1 frameshift, whereas the ORFs 2 through 11 were expressed by a set of subgenomic (sg) RNAs 3'-co-terminal (Hilf et al., 1995; Karasev et al., 1995). Later, an infectious cDNA clone of the full T36 genome, or an infectious minireplicon containing the 5'- and 3'-UTRs, the ORFs 1a and 1b, and variable portions of the central regions, were used to discover the elements necessary for CTV replication, gene expression and virus-host interactions, and to develop a CTV-based viral vector (Dawson et al., 2013, 2015; Folimonov et al., 2007; Gowda et al., 2003; Satyanarayana et al., 1999, 2001, 2002).

The sequence of the VT isolate from Israel confirmed very soon the genomic organization observed previously and showed an asymmetric distribution of variation along the genome, suggesting recombination events (Mawassi et al., 1996). A first result of the collaboration between the IBMCP and IVIA groups, and the William Dawson's lab at the University of Florida, Lake Alfred, was obtaining the sequences of two CTV isolates (T385 from Spain and T30 from Florida) that, contrasting with the decline-inducing isolates T36 and VT, were essentially asymptomatic in all hosts (Albiach-Martí et al., 2000; Vives et al., 1999).

Unexpectedly, these two isolates that had not been in contact for at least 30 years had almost identical sequence, which was also found in other isolates from several countries, indicating that certain CTV genotypes may show a remarkable evolutionary stasis. On the other hand, sequence comparisons between the isolates T385, T36, VT and SY568 from California (Yang et al., 1999) further suggested recombination events in isolates T36 and SY568 (Vives et al., 1999). Recombination was later confirmed as an important evolutionary force shaping CTV populations (Martín et al., 2009). Sequence availability of T30/T385 and other CTV strains was helpful to study genetic diversity of CTV isolates (Harper, 2013) and also to engineer recombinant cDNA clones by exchanging T36 genes for their homologous derived from other strains to examine the effects on CTV pathogenicity (Albiach et al., 2010) or to analyze the mechanism of superinfection exclusion and cross protection between different CTV isolates (Folimonova, 2013).

5. Characterizing genetic variability in distal regions of the CTV genome

Analysis of the genetic variation among CTV isolates in the 5'- and 3'-terminal regions and in the *p23* gene revealed limited sequence variation in the 984 3'-terminal nt, with most isolates sharing more than 90% identity, whereas the 5'-UTR of some isolates showed as little as 44% identity (López et al., 1998). This variation, however, was not random, but all sequences analyzed could be assigned to one of three groups defined (I, II and III), with intra-group identity being higher than 88% in the three types and inter-group identity ranging between 44 and 64%. In spite of the wide sequence variation between groups, their predicted secondary structures of minimum energy were very similar and included two stem-loops (A and B), with most of the nucleotide changes being accommodated in the loops, and when occurring in the double-stranded (ds) stems, the general features being preserved by compensatory mutations. This conservation of the secondary structure by co-variation strongly suggested some role *in vivo* for it. Indeed, mutational analysis of the 5'-UTR using an infectious cDNA clone of the CTV T36 isolate and a smaller CTV replicon derived from it to infect *N. benthamiana* protoplasts showed that the secondary structure was more important for replication

than the primary structure. However, some compensatory mutations predicted to maintain the secondary structure and allowing normal replication levels, impaired virus passage to new protoplasts, indicating that the 5'-UTR contains sequences required for both replication and virion assembly (Gowda et al., 2003).

While searching for different types of 5'-UTR sequences it was observed that some CTV isolates contained sequences belonging to more than one group, suggesting that repeated inoculations might have occurred in field trees along the years (López et al., 1998). Further analysis of 57 isolates of different origin and pathogenic characteristics, using RT-PCR amplification with group-specific primer sets, showed that in 19 of them, only the type III sequence was detected, whereas the others contained mixtures of two or the three sequence types. While the isolates containing only the type III sequence caused mild or moderate symptoms in Mexican Lm, a sensitive indicator plant for CTV, pathogenic isolates causing SP in SwO or Gf usually contained mixed sequences including the type II (Ayllón et al., 2001). This association between type II 5'-UTR sequence and highly pathogenic isolates was further confirmed (Ruiz-Ruiz et al., 2006), suggesting that this gRNA region might have co-evolved with others directly involved in pathogenesis.

The genetic variation of the *p23* gene was further assessed by comparing the predominant sequence variants in the viral population of 18 CTV isolates of different geographic origin and pathogenicity characteristics, selected by single-strand conformation polymorphism (SSCP) analysis (Sambade et al., 2003). Phylogenetic analysis of these sequences showed three groups of isolates: one included only mild isolates, other clustered severe isolates causing SP on Gf and/or SwO, and the third comprised loosely associated isolates producing variable symptoms. The first two groups showed low within-group genetic diversity values, much higher between-group diversity and no evidence for recombination in most isolates, whereas the third group was more variable and most isolates included recombination events.

Amino acid (aa) comparisons between the p23 proteins of the 18 isolates showed an interesting region between aa positions 50 and 86 that comprises several basic residues (positions 50-67) and a putative zinc-finger motif (positions

68-86) that suggested potential RNA-binding activity (see below) (Fig. 2). While the residues important for this activity (the basic aas and the Cys and His residues coordinating the Zn ion) were conserved in all isolates, sequence differences separating the three groups of isolates affected some positions in their close vicinity. Although association of p23 and symptom expression could result from co-evolution with other genome regions responsible for pathogenicity, direct involvement of p23 in CTV pathogenicity was later documented (see below).

6. Characterizing p23: a CTV-specific multifunctional protein

Early studies on the structure and expression of the CTV genome suggested that the p23 protein encoded by ORF 11 had some peculiarities suggestive of an important role in CTV biology. The narrow natural host range of CTV, essentially restricted to the genus *Citrus* and some close relatives, and the absence of p23-homologs in other closteroviruses (Dolja et al., 2006; Pappu et al., 1994) suggested that this protein might have evolved to regulate specific interactions between CTV and citrus (Flores et al., 2013). The ORF11 is adjacent to the 3'-UTR in the CTV gRNA, and its corresponding sgRNA is the second more abundant in infected tissues (Hilf et al., 1995). Also, in CTV-inoculated *N. benthamiana* and citrus protoplasts, the p23-sgRNA accumulated earlier than the other sgRNAs and was the most abundant in the first stages and the second later. Moreover, time-course analysis of the gRNA and sgRNAs accumulation showed that most sgRNAs increased in parallel with the gRNA along 2-5 days post-inoculation (dpi), except for the smallest sgRNA, encoding the p23 protein, that increased earlier (Navas-Castillo et al., 1997). Although the p23 sequence did not have significant similarity with other proteins in databases (Pappu et al., 1994), the presence of a cluster of positively charged aa residues and two conserved Cys residues, also observed in RNA-binding proteins encoded at the 3' end of the genome of different positive-stranded RNA viruses (Koonin et al., 1991), suggested that p23 could also be an RNA-binding protein involved in the regulation of CTV expression (Dolja et al., 1994). As with some of these proteins, p23 was also detected in the cytoplasmic

fraction of infected cells (Pappu et el., 1997). These data induced the IBMCP-IVIA team to further characterize the p23 protein, its cellular location and its interactions with host factors to better understand its role in CTV biology.

6.1. P23 is an RNA-binding protein that regulates asymmetrical accumulation of (+) and (-) RNA strands

To examine if p23 actually was an RNA-binding protein it was expressed in *Escherichia coli* fused to the maltose binding protein and purified by affinity chromatography (López et al., 2000). Gel retardation and UV crosslinking assays demonstrated that p23 cooperatively binds ssRNA in a non-sequence-specific mode. The p23-RNA complex remains stable at high salt concentrations, suggesting that interactions other than those between basic motifs of p23 and the negatively charged RNA are involved. Competition assays showed that the affinity of p23 for ssRNA and dsRNA was similar and clearly higher than for ss- or dsDNA. Mutational analysis mapped the RNA-binding domain of p23 between aa positions 50 and 86, containing the putative zinc-finger motif and several basic aas (Fig. 2). Elimination of the conserved residues presumably involved in coordinating the zinc ion did not abolish RNA-binding activity, but the apparent dissociation constant increased in comparison with the wild p23, suggesting that these conserved aas might provide increased specificity or stability *in vivo*.

Confirmation of the importance of p23 as a regulatory protein in CTV genome expression arrived very soon when Satyanarayana et al. (2002) observed that CTV-infected protoplasts accumulated in parallel positive and negative strands of both gRNA and sgRNAs, but the plus-to-minus ratio for these RNAs was about 10 to 20:1 and 40 to 50:1, respectively. However, when protoplasts were inoculated with a deletion mutant lacking all the 3' genes, it replicated efficiently, but produced plus and minus strands at a greatly reduced ratio (about 1 to 2:1). Analysis of mutants containing each of the 3'-proximal genes revealed that expression of *p23* controlled asymmetrical RNA accumulation. A frameshift mutation after the fifth codon of *p23* resulted in nearly symmetrical accumulation, indicating that it was the p23 protein, not a *cis*-acting element within the *p23* sgRNA, that controlled

asymmetrical accumulation of CTV RNAs. Moreover, in-frame deletion mutants of *p23* showed that the N-terminal 5 to 45 and the C-terminal 181 to 209 aa residues were not required to control asymmetrical RNA accumulation, whereas the residues 46 to 180, including the basic and zinc-finger domains, were indispensable. Also, changing the conserved cysteine residues to alanine in the zinc-finger motif abolished p23 activity, suggesting direct involvement of the zinc-finger in asymmetrical RNA accumulation. The p23 control of RNA accumulation seems to be exerted by downregulating negative-RNA accumulation with little increase of positive stranded RNA, which indirectly favors expression of 3' genes.

6.2. P23 is an intracellular suppressor of RNA silencing

CTV-infected citrus plants accumulate, in addition to gRNA, sgRNAs and defective RNAs, high amounts of virus-derived small RNAs (vsRNAs) (Fagoaga et al., 2006). These belong to a broader class of small RNAs (sRNAs) – including small interfering RNAs (siRNAs) of 21, 22, and 24 nt and micro RNAs (miRNAs) of 21 and 22 nt – produced by RS, a regulatory mechanism that modulates expression of host genes and protect the host from invading nucleic acids, both foreign (viruses, viroids and transgenes) and endogenous (transposons). RS is triggered by dsRNAs or snap-folded ssRNAs that are cleaved by some RNase III isozymes (Dicer or Dicer-like, DCL) and processed to sRNAs. Upon sRNAs incorporation into an RNA inducing silencing complex (RISC), these sRNAs guide specific Argonaute (AGO) proteins for sequence-specific inactivation o their cognate DNAs or RNAs at the transcriptional or post-transcriptional level, respectively (Mallory and Vaucheret, 2010). To overcome this mechanism viruses have evolved to encode RNA silencing suppressors (RSS) that interfere one or more of the silencing steps (Csorba et al.,2009; Ding, 2010). Since the antiviral branch of RS may overlap with the branch regulating plant homeostasis via miRNA and siRNAs, the RSS counter-defense system may act on both branches and produce some of the developmental alterations observed in virus-infected plants (Jay et al., 2011).

Analyses of the CTV 3'-proximal genes as potential expressors of RSS, using the transgenic line 16c of *N. benthamiana* that constitutively expresses the green fluorescent protein (GFP), and the transgenic tobacco line 6b5 that carries the beta-glucuronidase (GUS) gene permanently silenced, revealed that p23 suppresses just intracellular silencing and p25 just intercellular silencing, whereas p20 shows both types of silencing (Lu et al., 2004). Thus, CTV has evolved a sophisticated viral counter-defense acting on several steps of the antiviral silencing route.

To get a deeper insight on the silencing response induced by CTV in citrus plants, the sRNA patterns of CTV-infected and mock-inoculated plants were examined by gel-blot hybridization, deep sequencing (Solexa-Illumina) and bioinformatic data analyses in young bark of two highly susceptible (Mexican Lm and SwO) and one partially resistant (SO) hosts (Ruiz-Ruiz et al., 2011). The results obtained show that CTV-derived sRNAs: i) are abundant (more than 50% of the total sRNAs) in the two susceptible hosts that accumulate high virus titer, but not in SO (only 3.5% of the total sRNAs), which shows lower CTV titer, ii) have a predominant size of 21-22 nt, with over-accumulation of those of (+) polarity, and iii) derive from the whole CTV genome, allowing its complete assembly from viral sRNA contigs, but display an asymmetrical distribution with a prominent hotspot spanning the 3'-terminal 2500 nt (Fig. 3). These results indicate a strong antiviral response in the most susceptible hosts (Lm and SwO) and a more limited reaction in the partially resistant SO, with the citrus homologues of DCL2 and DCL4 ribonucleases mediating the generation of the 22 and 21 nt sRNAs. The asymmetrical distribution of virus-derived sRNAs along the CTV genome suggests that these ribonucleases act on the ds forms of both the gRNA and sgRNAs. The plant-derived sRNA profile was similar in the three mock-inoculated controls, with the 24-nt sRNAs being predominant, however, while this profile was little affected by CTV infection in SO, the susceptible hosts (Lm and SwO) showed a significant reduction of the 24-nt sRNAs.

6.3. P23 increases CTV accumulation in SO and abolish virus restriction to the phloem

An infectious cDNA clone of the T36 CTV isolate from Florida was engineered to build up a virus vector expressing GFP in the infected cells that allowed monitoring virus distribution in infected plants (Folimonov et al., 2007). Inoculation of alemow (*C. macrophylla* Wester), a highly CTV-susceptible host, and SO, which is partially resistant, with CTVT36-GFP showed abundant infection foci comprising multiple cells in the alemow phloem, whereas the SO phloem had few foci, all formed by single cells. This suggested lack of cell-to-cell movement in SO, with the virus relying only in the long-distance movement to invade the plant (Folimonova et al., 2008), a hypothesis supported by previous observation that protoplasts from SO or from the CTV-resistant TfO accumulate as much CTV virions as protoplasts from susceptible hosts (Albiach-Martí et al., 2004, and personal communication).

To gain a deeper insight into this peculiar CTV-host interaction, transgenic plants of SO and of SwO (also a highly susceptible host) expressing p23, or transformed with an empty vector as control, were graft-inoculated with the CTV isolate T385 or with the GFP-expressing T36 vector (Fagoaga et al., 2011). While p23-expressing and control SwO plants accumulated similar virus levels, the viral load in SO plants expressing p23 was 10-10^5 times higher than in the corresponding control plants. Also, contrasting with the single-cell infection foci detected in the phloem of the control SO plants, a higher number of foci including 2-6 infected cells were observed in p23-expressing SO plants, indicating cell-to-cell movement of the virus (Fig. 4). On the other hand, in p23-expressing SwO and SO plants CTV infection was not restricted to the phloem, since GFP-produced fluorescence was observed in mesophyll protoplasts and cells from infected transgenic plants, but not in cognate protoplasts and cells from the control plants. Overall, these results indicate that, when ectopically expressed, p23 promotes CTV escaping from the phloem and also facilitates systemic infection of the partially resistant SO. The distinct reaction in SwO and SO suggests a differential interaction between p23 and other viral- and host-encoded factors to transverse diverse cell boundaries. While CTV titer increase promoted by p23 in SO may be

associated in part with its RSS activity, the CTV exit from the SwO and SO phloem is likely mediated by a different p23 function related to virus movement. This hypothesis is supported by finding that one of the cell targets for p23 accumulation is precisely plasmodesmata (see below).

6.4. P23 also has suppressor activity of the basal defense system mediated by salicylic acid (SA)

Although ectopic expression of p23 increased CTV titer in SO, the following data indicated that RS was not the only factor involved in partial resistance of this host: i) while in CTV-susceptible hosts like SwO or Mexican Lm the highest virus accumulation was observed in the first flush after inoculation, in SO the virus titer increased in successive flushes along 2 years, depending on the CTV isolate (Comellas, 2009), ii) in susceptible hosts, CTV-derived siRNAs were detected in the first flush after inoculation, whereas in SO detection was achieved only one year later, likely due to the need for a threshold virus titer to trigger RS (Comellas, 2009), and iii) while in susceptible hosts CTV-derived siRNAs amounted to 53.3% of the total sRNAs detected by deep sequencing, in SO this fraction was only 3.5% (Ruiz-Ruiz et al., 2011). These data suggest that, at least in the initial stage after inoculation, resistance of SO does not totally depend on the RS response, but perhaps the SA-mediated defense system plays an important role.

To gain insight on factors involved in SO resistance to CTV, the role of several genes involved in the SA-signaling and RS defense pathways was examined by blocking their expression using virus-induced gene silencing (VIGS) with a virus vector for citrus based on *Citrus leaf blotch virus* (CLBV) (Agüero et al., 2012). For this purpose, segments of the selected endogenous plant genes (RNA-dependent RNA polymerase 1, *RDR1*, non-expressor of pathogenesis-related genes 1, 3 and 4, *NPR1*, *NPR3/NPR4*, and *DCL2/DCL4*) were inserted in the vector, between the 3' end of the coding region and the 3'UTR. RDR1 is involved in virus resistance mediated by both the SA-signaling and the RS pathways and its expression in citrus appears up-regulated after CTV infection (Gandía et al., 2007). The NPR1 protein regulates the SA-signaling pathway (Wu et al., 2012): its accumulation is

needed for expression of the basal defense genes, but later, its turnover is necessary for systemic acquired resistance (SAR). The NPR3 and NPR4 proteins mediate NPR1 degradation and are associated with the hypersensitive reaction (Fu et al., 2012). Finally, as indicated above, DCL2 and DCL4 are the enzymes responsible for generation of virus-derived siRNAs in the RS pathway (García-Ruiz et al., 2010). The recombinant CLBV vector was agroinoculated in *N. benthamiana* plants to produce virions, these virions were mechanically transmitted to RL seedlings, and these plants were later used as inoculum source to graft-inoculate SO or new RL plants for VIGS. Silenced and control plants infected with the wild type CLBV were graft-inoculated with CTV and monitored for CTV accumulation (Gómez-Muñoz et al., 2017).

Silencing the genes *RDR1*, NPR1 or *DCL2/DCL4* increased CTV spread and accumulation in SO plants in comparison with the non-silenced controls, suggesting that both the SA-signaling and the RS pathways are involved in SO resistance. Contrarily, silencing the genes *NPR3/NPR4* slightly decreased CTV titer in SO, likely as a result of higher NPR1 accumulation that would enhance the basal plant resistance.

On the other hand, comparative analysis of SO plants inoculated with the symptomless isolate T385, the moderate isolate T36 (inducing mild SY) and the severe isolate T318, (causing severe stunting and SY in SO) showed that i) while T318 or T36 accumulated more in the shoots than in the roots, the opposite was true for T385, and ii) symptom intensity did not correlate with virus accumulation (Comellas, 2009). Because plant viruses encode RSS proteins that suppress RS- or SA-responsive signaling to avoid the plant defense system (Laird et al., 2013), the different viral load and tropism observed between CTV isolates in SO plants could be due to different ability of their RSS proteins (p25, p20 and p23) to suppress the SA-signaling pathway. This ability was compared by two *Agrobacterium*-mediated transient assays: one based on the capacity of SA suppressors to delay cell death triggered by a gene-for-gene interaction, and the other, based on measuring reduced expression of the pathogenicity related protein 1a (PR1a) after SA silencing (Laird et al., 2013).

In the first, the protein p19 from *Tomato bushy stunt virus* (TBSV), inciting an SA-dependent hypersensitive reaction (HR) on leaves of *N. tabacum* Xanthi (Angel and Schoelz, 2013), was co-expressed in this plant with p25, p20 or p23 from each CTV isolate, using as positive control the p6 protein from *Cauliflower mosaic virus* (CaMV), and the empty vector as negative control. The p20 or p23 proteins from either isolate delayed cell death in comparison with the negative control, with p20 being a more efficient HR suppressor than p23. Also, p20 and p23 from isolate T318 were slightly more suppressive than their homologs from T36 or T385, with the latter being the less suppressive (Gómez-Muñoz et al., 2017).

In the second procedure, agroinoculation of *N. benthamiana* plants with a binary plasmid triggered expression of the gene *PR1a*, a response that can be suppressed by transient expression of RSSs (Laird et al., 2013). Thus, the amount of *PR1a* mRNA, estimated by RT-qPCR, was compared in plants agroinoculated with empty pCAMBIA or pCAMBIA expressing p25, p20 or p23 from each of the three CTV isolates. *PR1a* mRNA accumulation was drastically reduced in plants expressing p20 or p23 from the three CTV isolates, but activity of p20 and p23 from the T318 and T36 was stronger than that observed with their homologs from T385. These results indicate that p20 and p23 have suppressor activity of the SA-signaling pathway, and that this activity is more intense for proteins from the more virulent isolates (Gómez-Muñoz et al., 2017).

In summary, the initial resistance of SO to CTV accumulation likely results from the SA-mediated defense deployed by this host, rather than from RS, albeit other antiviral pathways cannot be excluded. Also, variable accumulation and tropism of CTV isolates in SO could be associated to the different capacity of their p20 and p23 proteins to suppress the SA-signaling pathway in this host.

6.5. P23 is targeted to the nucleolus and plasmodesmata

Because subcellular localization of a protein may give clues on its biological function, the p23-GFP fusion was agro-expressed in *N. benthamiana* and the infiltration halos were examined for GFP fluorescence by confocal laser-scanning microscopy. The fluorescence spots indicated that p23 preferentially accumulated

494 in the nucleolus and Cajal bodies, and in punctuated structures in the cell wall
495 resembling plasmodesmata, a result that was further confirmed in co-expression
496 experiments with proteins specifically marking the nucleolus (fibrillarin) and the
497 plasmodesmata (the movement protein of an ilarvirus). These findings suggested
498 that p23 should contain a nucleolar localization signal (NoLS) and a
499 plasmodesmata localization signal (PLS). NoLS are usually formed by short motifs
500 rich in basic aas, a type of structure previously observed in p23. To assess if these
501 p23 structures were part of its NoLS, seven truncated and 10 point-mutated
502 versions of p23 fused to GFP were assayed for fluorescence localization. Deletion
503 mutants showed that regions 50-86 and 100-157 (excluding the fragment 106-114),
504 both with basic motifs and the first with a zinc-finger motif, contain what appears to
505 be a bipartite NoLS. The alanine substitution mutants further delimited this motif to
506 three cysteines of the zinc-finger and some basic aas. On the other hand, all
507 deletion mutants, but the one lacking aas 158-209, lost their PLS (Ruiz-Ruiz et al.,
508 2013).
509 As indicated above, p23 acts as an intracellular RSS when co-agroexpressed
510 with GFP under the control of the CaMV 35S promoter in the transgenic line 16c of
511 *N. benthamiana*, constitutively expressing GFP (Lu et al., 2004). In leaves co-
512 infiltrated with the plasmids 35S-p23 and 35S-GFP fluorescence was intense for
513 about one week, whereas in those infiltrated only with 35S-GFP, or co-infiltrated
514 with either the control empty vector or with any of the 17 plasmids carrying the *p23*
515 deletion or substitution mutants (except the alanine substitution mutant affecting
516 the histidine of the predicted zinc-finger) almost no fluorescence was observed.
517 Moreover, highly fluorescent leaves accumulated high level of *gfp* mRNA and low
518 level of *gfp*-derived siRNA, as detected by gel blot hybridization with a *gfp*-specific
519 riboprobe, whereas the opposite was true for RNA extracts from non-fluorescent
520 leaves. Overall, these results indicate that the p23 RSS activity may be related to
521 its nucleolar localization, and that this activity involves most p23 regions (Ruiz-Ruiz
522 et al., 2013).
523
524 **6.6. P23 is involved in CTV symptom expression of citrus plants**

525 Before its role as RSS was discovered p23 was associated with pathogenicity
526 characteristics of CTV isolates (Pappu et al., 1997; Sambade et al., 2003). Also,
527 ectopic expression of p23 from the T36 isolate in Mexican Lm under the control of
528 the 35S promoter incited phenotypic aberrations (intense vein clearing, epinasty
529 and yellow pinpoints in leaves, SP, young shoot necrosis and collapse), more
530 intense than those caused by CTV infection in non-transgenic plants, whereas
531 control plants transgenically expressing a truncated version of p23 remained
532 symptomless (Fig. 5 A,B,E). Thus, onset of CTV-like symptoms was associated
533 with expression of the p23 protein. Indeed, symptom intensity paralleled the level
534 of protein accumulation (Ghorbel et al., 2001). When this experiment was repeated
535 using p23 from T317 (Fig. 5 C,D), a mild CTV isolate that usually is asymptomatic
536 or incites only mild vein clearing in Mexican Lm, again the control plants
537 transformed with a truncated version of *p23* looked normal, whereas those
538 expressing the p23 protein displayed symptoms very similar to those incited by p23
539 from the moderate isolate T36. In comparison with non-transgenic plants infected
540 with CTV, transgenic Lm accumulates higher levels of p23 and this is not restricted
541 to phloem cells (Fagoaga et al., 2005), two factors that might explain the presence
542 of non-specific aberrations not observed in natural CTV infections.
543 Transformation of the CTV-susceptible SwO, the resistant TfO and the partially
544 resistant SO with the *p23* gene from T36 also incited phenotypic aberrations, some
545 of them resembling CTV symptoms, even though graft-inoculation of non-
546 transgenic plants with CTV T36 is symptomless in SwO, incites only the SY
547 syndrome in SO, and do not produce a detectable infection in TfO. Contrarily,
548 transgenic plants of *N. benthamiana* and *N. tabacum* accumulated p23 without
549 detectable phenotypic aberrations, suggesting that interference of p23 in plant
550 development could be citrus-specific (Fagoaga et al., 2005). Later, it was
551 discovered that CTV T36 not only replicated in *N. benthamiana* protoplasts, but it
552 could also systemically infect complete plants of this species agroinoculated with
553 an infectious cDNA clone of this isolate and appropriate RSSs. Systemically
554 infected plants accumulated a high virus load, displayed symptoms (mainly
555 stunting, epinasty, crumpled new leaves, vein clearing, and necrosis of medium

and upper leaves) and usually collapsed and died after 2 to 4 months post-inoculation (Fig. 5 F) (Ambrós et al., 2011).

The above results raised several questions on the pathogenic activity of p23 in *N. benthamiana* and in citrus. Firstly, contrasting with citrus species, ectopic expression of p23 in *N. benthamiana* and *N. tabacum* was asymptomatic despite i) p23 accumulating at similar levels in citrus and in *Nicotiana* (Fagoaga et al., 2005), ii) p23 acting as RSS in both *Nicotiana* species (Lu et al., 2004), and iii) CTV T36 inducing symptoms in systemically infected *N. benthamiana* leaves (Ambrós et al., 2011). This differential response might be due to insufficient p23 accumulation to induce developmental aberrations in transgenic *N. benthamiana* plants. If so, could expression from a viral vector overcome the p23 threshold to incite these aberrations? Also, could the p23 region responsible for pathogenicity be delimited by this new expression system? Is the same p23 region responsible for symptoms in citrus and in *N. benthamiana*? On the other hand, because CTV infecting citrus is restricted to the phloem, some of the phenotypic aberrations observed after constitutive p23 expression in transgenic Lm might be just pleiotropic effects from expressing this protein in non-phloem cells. If so, expressing p23 under the control of a phloem-specific promoter from *Commelina yellow mottle virus* (CoYMV) (Medberry et al., 1992) could provide a more accurate picture of its pathogenic activity. Could this new expression system better mimic symptoms of natural CTV infections? If so, would it reproduce the distinct syndromes caused by infection with the T36 and T317 isolates?

6.6.1. The 157 N-terminal aas of p23 are involved in symptom expression of both *N. benthamiana* and citrus plants

To answer the first group of questions, p23 from CTV T36 was expressed in *N. benthamiana* as a sgRNA of *Potato virus X* (PVX) (Voinnet et al., 1999). Although appearance of the leaves mechanically inoculated with the wild type PVX or its recombinant version (PVX-p23) remained unaltered, the upper non-inoculated leaves of both treatments showed vein clearing and a mild chlorotic mosaic at 7 dpi. However, at 10 dpi, symptoms of the plants inoculated with PVX remained

587 unchanged, whereas plants inoculated with PVX-p23 showed stunting and necrotic
588 mottling in systemically infected leaves and stems and at 15 dpi the plants died,
589 indicating that p23, like other RSS, is a pathogenicity determinant in *N.*
590 *benthamiana*. Furthermore, expression of the fusion p23-GFP from PVX confirmed
591 its nucleolar localization. When the 17 mutants previously agroinoculated in plants
592 to search for determinants of p23 subcellular localization (see above) were
593 expressed from the PVX vector, only the deletion mutant lacking the 158-209 aas
594 and the alanine substitution mutant of the histidine 75 incited symptoms similar to
595 those observed with the wild type p23. These results indicate that the pathogenic
596 determinant of p23 in *N. benthamiana* is located in the 157 N-terminal aas, with the
597 zinc-finger motif and the flanking basic aas being part of this determinant. Also, the
598 RSS activity and the capacity to induce symptoms must be independent functions
599 of p23, since deletion of the 158-209 aas abolished the RSS activity, but retained
600 pathogenicity (Ruiz-Ruiz et al., 2013).
601 The effects of viral proteins in the natural host plants (particularly in woody
602 plants) and in experimental hosts like *N. benthamiana* may not be necessarily
603 identical. Because p23 induces CTV-like symptoms when ectopically expressed in
604 Mexican Lm and other citrus species (Fagoaga et al., 2005; Ghorbel et al., 2001),
605 the next question to answer was whether similar p23 regions were involved in
606 pathogenicity in both citrus and *N. benthamiana*. To this end, the p23 protein from
607 T36 and three truncated versions thereof, lacking aas 100-209, 158-209 and 50-
608 86, under the control of the CaMV 35S promoter were used to transform Mexican
609 Lm plants. While expression of the first mutant in transgenic Lm did not induce
610 phenotypic aberrations, expression of the second, comprising the 157 N-terminal
611 aas, incited CTV-like leaf symptoms and SP similar to, albeit milder than, those
612 elicited by the complete p23 protein. Moreover, deletion of aas 50-86 also
613 abolished induction of developmental aberrations, thus demarcating the p23 region
614 responsible for pathogenesis to a 157 aas fragment including the zinc-finger motif
615 and flanking basic aas. Overall, these results support the idea that similar p23
616 regions are responsible for pathogenesis in citrus and *N. benthamiana*, and
617 therefore, that results obtained in this manageable experimental host may serve, at

least in part, to predict results with the less workable system of transgenic citrus.

6.6.2. Phloem-restricted expression of p23 in citrus reproduces specific CTV symptoms

To answer the questions related to phenotypic aberrations observed in transgenic citrus constitutively expressing p23, the *p23* genes from the severe T36 and the mild T317 CTV isolates were expressed in transgenic Lm plants under the control of a phloem-specific (from CoYMV) or a constitutive (35S from CaMV) promoter. Expression of p23 restricted to the phloem reproduced the CTV-specific symptoms (vein clearing and necrosis and SP), but not the non-specific aberrations (mature leaf epinasty, yellow pinpoints, apical necrosis and growth cessation) observed when p23 was ectopically expressed. Moreover, vein necrosis and SP were observed in plants expressing p23 from T36, but not from T317, thus reproducing symptoms displayed by non-transgenic plants infected with those CTV isolates. Phloem-specific expression of a deletion mutant of p23 (T36) lacking aas 158-209 was able to induce the same CTV-like symptoms, further supporting that the region comprising the 157 N-terminal aas is responsible, at least in part, for the vein clearing, SP and, possibly, vein necrosis in Mexican Lm (Soler et al., 2015). The intensity of SP in alemow, also a CTV-sensitive host, seems to be modulated by the combined expression of three CTV genes (p33, p18 and p13) that are dispensable for systemic infection of this host (Tatineni et al., 2011, 2012).

Finally, a role for p23 in causing the SY syndrome in SO and Gf was also proved using a different approach. Virions from an infectious cDNA clone of the SY-inducing isolate T36 (Satyanarayana et al., 1999, 2001), in which the 3'-terminal region, including the gene *p23* and the 3'-UTR, was changed for its homologous derived from the non-SY isolate T30, were inoculated in SO or Gf. While control plants inoculated with the wild T36 showed SY, those infected with the recombinant virions remained symptomless, indicating that the exchanged region contains the pathogenic motif inducing SY (Albiach-Martí et al., 2010).

6.7. Ectopic expression of p23 and the other RSSs provides partial

protection against CTV infection mediated by RS

Because p23 is a regulatory protein, it seemed a good candidate to interfere CTV replication by RS in p23-expressing transgenic citrus plants. Indeed this was the primary objective of citrus transformation with the *p23* gene (Fagoaga et al., 2005; Ghorbel et al., 2001). Although most transgenic lines obtained showed developmental aberrations, a few of them remained symptomless and showed traits characteristic of RS (multiple copies of the transgene, low level of the cognate mRNA and accumulation of *p23*-derived siRNAs, and transgene methylation). When propagations of these silenced lines were graft- or aphid-inoculated with CTV T36, some of them appeared immune (they did not display symptoms neither accumulated CTV virions or viral RNA), others showed moderate resistance (they showed delayed infection and attenuated symptoms in comparison with control plants transformed with an empty vector), and still others were fully susceptible (with symptom intensity and virus accumulation similar to those of the control plants). This variable response of clonal propagations from the same transformed line indicated that factors other than genetic background (perhaps the developmental stage) must be important for RNA-mediated resistance to CTV (Fagoaga et al., 2006).

Because RS is triggered by dsRNA, this plant response can be improved by transformation with sense and antisense sequences separated by an intron, a construct known as intron-hairpin design (ihp). Upon transcription of this transgene type, the resulting hairpin RNA function as a strong silencing inducer (Smith et al., 2000). In an attempt to improve resistance to CTV, Mexican Lm plants were transformed with the 3'-terminal 549 nt, comprising the 3'-UTR and part of the *p23* gene, in sense, antisense or ihp mode, and then examined for transgene-derived siRNAs accumulation and symptoms after inoculation with CTV T36. All propagations from the sense, antisense and empty-vector (control) transgenic lines became infected, with the exception of a single sense-line plant (out of seven). Contrastingly, 9 out of 30 ihp lines showed partial resistance, with 9-56% of their propagations, depending on the line, remaining uninfected and the others being susceptible. Although resistance was always associated with the presence of

transgene-derived siRNAs, their accumulation level was variable and it did not parallel their degree of resistance. Moreover, examination of transgenic ihp lines with a single transgene integration (to make comparison easier) revealed that resistance to CTV was better correlated with low accumulation of the transgene-derived transcripts than with high accumulation of transgene-derived siRNAs, perhaps because only part of these siRNAs are able to complete the RS process (López et al., 2010).

These results and those from other groups (Batuman et al., 2006; Febres et al., 2008; Roy et al., 2006) indicate that developing transgenic resistance to CTV in citrus seems more difficult than in other virus-host systems, likely due to the complex host-virus interactions. Specifically, a strong citrus antiviral defense against CTV infection through RS, as illustrated by the high accumulation of CTV-derived sRNAs in infected plants (Fagoaga et al., 2006; Ruiz-Ruiz et al., 2011), counteracted by a sophisticated CTV defense system based on three RSS proteins. Thus, blocking CTV infection might require simultaneous silencing of the three RSS genes. Because the highest protection was previously obtained in transgenic plants expressing an ihp construct of the 549 3'-terminal nt, Mexican Lm plants were transformed with a vector carrying an ihp with full untranslatable versions of the genes *p25*, *p20* and *p23* plus the 3'-UTR (from the T36 isolate) (Soler et al., 2012). Three transgenic lines displayed complete resistance to CTV after graft-inoculation with the same virus isolate, with all the propagations remaining asymptomatic and virus-free. Accumulation of transgene-derived siRNAs was necessary, but not sufficient for CTV resistance. However, when propagations of the same three lines were inoculated with the heterologous CTV isolate T318A, with 91-92% nucleotide identity with T36 for the three genes, resistance was only partial, indicating a sequence-dependent resistance mechanism. These results confirmed that simultaneous silencing of the three RSS is critical for CTV resistance, albeit participation of other concomitant RS mechanism cannot be excluded. On the other hand, from a practical standpoint, resistance breakage by genetically divergent virus isolates would be a serious limitation for using CTV-resistant transgenic plants in the field. This problem might

711 be overcome using this same strategy with a chimeric ihp construct showing in the
712 three genes more than 95% nucleotide identity with all known CTV genotypes,
713 however, validity of this approach would need thorough testing.
714
715 **6.8. P23 interacts with different host factors to develop the CTV infectious**
716 **cycle**
717 Viral infection of a host plant requires multiple interactions between virus- and
718 host-encoded proteins to complete the different steps of the process (replication,
719 cell-to-cell movement and systemic invasion of the plant). Replication of RNA
720 viruses usually occur in the cytoplasm using membranous vesicles, called viral
721 replication complexes (VRC), which are assembled with host factors and virus-
722 encoded proteins (den Boon and Alquist, 2010). Viruses also encode movement
723 proteins that can bind to the VRC and mediate its association with plasmodesmata
724 and viral movement to neighbor cells or to phloem vessels (Heinlein, 2015).
725 Because p23 is a CTV-specific multifunctional protein, potential host factors
726 interacting with this protein were examined in *N. benthamiana*, a manageable
727 symptomatic experimental host for CTV. Yeast two-hybrid (Y2H) screening of an
728 expression library of this host identified glyceraldehyde 3-phosphate
729 dehydrogenase (GAPDH) as potential interactor with p23. Bimolecular
730 fluorescence complementation (BiFC) revealed that p23 interacts with itself in the
731 nucleolus, Cajal bodies and plasmodesmata, and with GAPDH, in the cytoplasm
732 and in plasmodesmata. The p23-GAPDH interaction was abolished in p23 deletion
733 mutants affecting the 157 N-terminal aas, including the zinc-finger motif and some
734 basic aas, but not in a mutant lacking the C-terminal 51 aas. Virus-induced gene
735 silencing of the GAPDH mRNA using a *Tobacco rattle virus* (TRV)-derived vector
736 caused accumulation of GAPDH-derived siRNAs and a concomitant reduction in
737 GAPDH mRNA. Agroinoculation of these silenced plants with CTV resulted in
738 significant reduction of CTV accumulation, as detected by real-time RT quantitative
739 PCR, in comparison with non-silenced controls, indicating that the p23-GAPDH
740 facilitates the CTV infection cycle (Ruiz-Ruiz et al., 2018).
741 Using a similar approach, it was later discovered that p23 also interacts with a

742 host protein of the family of the FK506-binding proteins (FKBP) (Yang et al., 2021).
743 Members of this family contain at least one binding domain for FK506 (a macrolide
744 antibiotic) and are frequent in plants, in which they play a role in a variety of cellular
745 processes, including stress response or chloroplast function (Gollan et al., 2012).
746 Y2H screening of a Mexican Lm expression library, using p23 as bait, revealed
747 interaction of p23 with a homolog of the FKBP17-2 protein from *Arabidopsis*
748 *thaliana*, whose function is still unclear. This p23/FKBP17-2 interaction was
749 confirmed by BiFC and subcellular localization analyses. In *N. benthamiana*,
750 individual transient expression of p23 and (Nb)FKBP17-2 ligated to fluorescent
751 indicators showed that, while p23 targeted plasmodesmata, (Nb)FKBP17-2
752 appeared in chloroplasts. However, when both proteins were co-expressed
753 (Nb)FKBP17-2 localization changed, with most fluorescent signals being displaced
754 from chloroplasts to plasmodesmata and cytoplasm. Co-localization of p23 and
755 NbFKBP17-2 in plasmodesmata, also confirmed by BiFC, suggests that p23 can
756 change subcellular localization of (Nb)FKBP17-2. Finally, knocking down
757 expression of NbFKBP17-2 in *N. benthamiana* decreased CTV accumulation,
758 suggesting that interaction of p23 with this protein facilitates the CTV infection
759 cycle, as previously observed with the p23/GAPDH interaction (Ruiz-Ruiz et al.,
760 2018).
761
762 **7. Final remarks and future prospects**
763 Our knowledge on CTV and on tristeza disease management has greatly
764 improved in the last fifty years, particularly after the first reliable method for virion
765 purification and characterization was developed (Bar-Joseph et al., 1972). Ricardo
766 Flores was an important contributor to these developments. Using cesium sulfate
767 instead of cesium chloride for gradient purification avoided the need for virion
768 fixation, thus providing biologically active virions, which was critical to establish the
769 etiology of tristeza disease, and later, to assay CTV viral vectors or mutants
770 obtained by genome manipulation. Obtaining the full genome sequence of CTV
771 isolates with different pathogenicity characteristics allowed sequence comparisons
772 and identification of genome regions potentially associated with virulence.

Special attention deserves the advances achieved in the knowledge of the structure and biological function of the p23 protein and its potential use to control CTV. This CTV-unique protein has been involved in multiple functions including regulation of plus and minus RNA strand accumulation, suppression of RS- and SA-mediated defense pathways of the plant, pathogenesis and virus movement. Preferential location of p23 includes the nucleolus and Cajal bodies, and plasmodesmata. The structural motifs required for its biological functions are almost coincident with those associated with its subcellular location, indicating that this localization must be critical for those functions. Although interaction of p23 with some viral (p33 and p25) and host (GAPDH and FKBP17-2) proteins have been documented, this is clearly an area that needs future attention, particularly interactions with viral proteins catalyzing replication or mediating movement, or different types of AGOs involved in the host RS response. Efforts should be also directed to examine potential interactions of p23 with RNAs of viral or host origin, like the sRNAs that mediate RS (Flores et al., 2013).

Finally, finding that transgenic expression of an ihp construct with untranslatable versions of *p25*, *p20* and *p23* provided full protection against CTV infection was an important breakthrough, even if this resistance is sequence-dependent. The possibility of obtaining general transgenic resistance by manipulating sequences so that the new transgene show at least 95% identity with the RSS genes of most CTV isolates deserves careful examination.

Author statement

Pedro Moreno: Conceptualization, writing the original draft and final revision. **Carmelo López, Susana Ruiz-Ruiz and Leandro Peña:** Writing-reviewing and editing, Visualization. **José Guerri:** Writing-reviewing and editing. All authors approved the final submitted version of the manuscript.

Declaration of Competing Interest

The authors report no declarations of interest.

Acknowledgements

This research did not receive any specific grant from funding agencies in the public, commercial, or not-for-profit sectors.

References

Agüero, J., Ruiz-Ruiz, S., Vives, M.C., Velázquez, K., Navarro, L., Peña, L., Moreno, P., Guerri, J., 2012. Development of viral vectors based on Citrus leaf blotch virus to express foreign proteins or analyze gene function in citrus plants. Mol. Plant-Microbe Interact. 25, 1326-1337. doi: 10.1094/MPMI-02-12-0048-R.

Albiach-Martí, M.R., Grosser, J.W., Gowda, S., Mawassi, M., Satyanarayana, T., Garnsey, S.M., Dawson, W.O., 2004. Citrus tristeza virus replicates and forms infectious virions in protoplasts of resistant citrus relatives. Mol. Breed. 14, 117-128. https://doi.org/10.1023/B:MOLB.0000038000.51218.a7.

Albiach-Martí, M.R., Mawassi, M., Gowda, S., Satyanarayana, T., Hilf, M.E., Shanker, S., Almira, E.C., Vives, M.C., López, C., Guerri, J., Flores, R., Moreno, P., Garnsey, S.M., Dawson, W.O., 2000. Sequences of citrus tristeza virus separated in time and space are essentially identical. J. Virol. 74, 6856-6865. doi: 10.1128/jvi.74.15.6856-6865.2000.

Albiach-Martí, M.R., Robertson, C., Gowda, S., Tatineni, S., Belliure, B., Garnsey, S.M., Folimonova, S.Y., Moreno, P., Dawson, W.O., 2010. The pathogenicity determinant of Citrus tristeza virus causing the seedling yellows syndrome is located at the 3'-terminal region of the viral genome. Mol. Plant Pathol. 11, 55-67. doi: 10.1111/j.1364-3703.2009.00572.x.

Ambrós, S., El-Mohtar, C., Ruiz-Ruiz, S., Peña, L., Guerri, J., Dawson, W.O., Moreno, P., 2011. Agro-inoculation of *Citrus tristeza virus* causes systemic infection and symptoms in the presumed non-host *Nicotiana benthamiana*. Mol. Plant-Microbe Interact. 24, 1119-1131. doi: 10.1094/MPMI-05-11-0110.

Angel, C.A., Schoelz, J.E., 2013. A survey of resistance to Tomato bushy stunt virus in the genus Nicotiana reveals that the hypersensitive response is triggered by one of three different viral proteins. Mol. Plant-Microbe Interact. 26, 240-248. doi: 10.1094/MPMI-06-12-0157-R.

Ayllón, M.A., López, C., Navas-Castillo, J., Garnsey, S.M., Guerri, J., Flores, R., Moreno, P., 2001. Polymorphism of the 5' terminal region of *Citrus tristeza virus* (CTV) RNA: Incidence of three sequence types in isolates of different origin and pathogenicity. Arch. Virol. 146, 27-40. doi: 10.1007/s007050170188.

Bar-Joseph, M., Garnsey, S.M., Gonsalves, D., 1979a. The closteroviruses: a distinct group of elongated plant viruses. Adv. Virus Res. 25, 93-168. doi: 10.1016/S0065-3527(08)60569-2.

Bar-Joseph, M., Garnsey, S.M., Gonsalves, D., Moscovitz, M., Purcifull, D.E., Clark, M.F., Loebenstein, G., 1979b. The use of enzyme-linked immunosorbent assay for detection of citrus tristeza virus. Phytopathology 69, 190-194. doi: 10.1094/Phyto-69-190.

Bar-Joseph, M., Loebenstein, G., Cohen, J., 1972. Further purification and characterization of threadlike particles associated with the citrus tristeza disease. Virology 50, 821-828. doi: 10.1016/0042-6822(72)90436-9.

Bar-Joseph, M., Marcus, R., Lee. R.F., 1989. The continuous challenge of citrus tristeza virus control. Annu. Rev. Phytopathol. 27, 291-316.

Bak, A., Folimonova, S.Y., 2015. The conundrum of a unique protein encoded by citrus tristeza virus that is dispensable for infection of most hosts yet shows characteristics of a viral movement protein. Virology 485, 86-95. doi: 10.1016/j.virol.2015.07.005.

Batuman, O., Mawassi, M., Bar-Joseph, M., 2006. Transgenes consisting of a dsRNA of an RNAi suppressor plus the 3′ UTR provide resistance to Citrus tristeza virus sequences in Nicotiana benthamiana but not in citrus. Virus Genes 33, 319-327. doi: 10.1007/s11262-006-0071-y.

Cambra, M., Moreno, P., Navarro, L., 1979. Detección rápida del virus de la "tristeza" de los cítricos (CTV) mediante la técnica inmunoenzimática ELISA-Sandwich. An. INIA, Ser. Prot. Veg. 12, 115-121.

Comellas, M., 2009. Estudio de la interacción entre naranjo amargo y el virus de la tristeza de los citricos. PhD Thesis, Universitat Politécnica de Valencia, Valencia.

doi: 10.4995/Thesis/10251/7323.

Csorba, T., Pantaleo, V., Burgyán, J., 2009. RNA silencing: an antiviral mechanism. Adv. Virus Res. 75, 35-71. doi: 10.1016/S0065-3527(09)07502-2.

Dao, T.N.M., Kang, S.H., Bak, A., Folimonova, S.Y., 2020. A non-conserved p33 protein of Citrus tristeza virus interacts with multiple viral partners. Mol. Plant-Microbe Interact. 33, 859-870. https://doi.org/10.1094/MPMI-11-19-0328-FI

Dawson, W.O., Bar-Joseph, M., Garnsey, S.M., Moreno, P., 2015. Citrus tristeza virus: making an ally from an enemy. Annu. Rev. Phytopathol. 53,137-55. https://doi.org/10.1146/annurev- phyto-080614-120012.

Dawson, W.O., Garnsey, S.M., Tatineni, S., Folimonova, S.Y., Harper, S.J., Gowda, S., 2013. Citrus tristeza virus-host interactions. Front. Microbiol. 4, 88. https://doi.org/10.3389/fmicb.2013.00088.

den Boon, J.A., Ahlquist, P., 2010. Organelle-like membrane compartmentalization of positive-strand RNA virus replication factories. Annu. Rev. Microbiol. 64, 241-256. doi: 10.1146/annurev.micro.112408.134012.

Ding, S.W., 2010. RNA-based antiviral immunity. Nat. Rev. Immunol. 10, 632-644. doi: 10.1038/nri2824.

Dolja, V.V., Karasev, A.V., Koonin, E.V., 1994. Molecular biology and evolution of closteroviruses: Sophisticated build-up of large RNA genomes. Annu. Rev. Phytopathol. 32, 261-285.

Dolja, V.V., Kreuze, J.F., Valkonen, J.P., 2006. Comparative and functional genomics of closteroviruses. Virus Res. 117, 38-51. doi: 10.1016/j.virusres.2006.02.002.

Fagoaga, C., López, C., Hermoso de Mendoza, A., Moreno, P., Navarro, L., Flores, R., Peña, L.,2006. Post-transcriptional gene silencing of the p23 silencing suppressor of *Citrus tristeza virus* confers resistance to the virus in transgenic Mexican lime. Plant Mol. Biol. 60, 153-165. doi: 10.1007/s11103-005-3129-7.

887 Fagoaga, C., López, C., Moreno, P., Navarro, L., Flores, R., Peña, L., 2005. Viral-
888 like symptoms induced by ectopic expression of the *p23* gene of *Citrus tristeza*
889 *virus* are citrus specific and do not correlate with the pathogenicity of the virus
890 strain. Mol. Plant-Microbe Interact. 18, 435-445. doi: 10.1094/MPMI-18-0435.

891 Fagoaga, C., Pensabene-Bellavia, G., Moreno, P., Navarro, L., Flores, R., Peña,
892 L., 2011. Ectopic expression of the p23 protein of Citrus tristeza virus differentially
893 modifies viral accumulation and tropism in two transgenic woody hosts. Mol. Plant
894 Pathol. 12, 898-910. doi: 10.1111/j.1364-3703.2011.00722.x.

895 Fawcett, H.S., Wallace, J.M., 1946. Evidence of the virus nature of citrus quick
896 decline. Calif. Citrograph 32, 88-89.

897 Febres, V.J., Lee, R.F., Moore, G.A., 2008. Transgenic resistance to Citrus tristeza
898 virus in grapefruit. Plant Cell Rep. 27, 93-104. doi: 10.1007/s00299-007-0445-1.

899 Flores, R., Garro, R., Conejero, V., Cuñat, P., 1975. Purificación en gradiente de
900 densidad de sulfato de cesio de las partículas nucleoproteicas asociadas a la
901 tristeza de los cítricos. Rev. Agroquím. Tecnol. Alim. 15, 93-97.

902 Flores, R., Ruiz-Ruiz, S., Soler, N., Sánchez-Navarro, J., Fagoaga, C., López, C.,
903 Navarro, L., Moreno, P., Peña, L., 2013. Citrus tristeza virus p23: a unique protein
904 mediating key virus-host interactions. Front. Microbiol. 4, 98. doi:
905 10.3389/fmicb.2013.00098.

906 Folimonov, A.S., Folimonova, S.Y., Bar-Joseph, M., Dawson, W.O., 2007. A stable
907 RNA virus-based vector for citrus trees. Virology 368, 205-216. doi:
908 10.1016/j.virol.2007.06.038.

909 Folimonova S.Y., 2013. Developing an understanding of cross-protection by Citrus
910 tristeza virus. Front. Microbiol. 4, 76. https://doi.org/10.3389/fmicb.2013.00076.

911 Folimonova, S.Y., Folimonov, A.S., Tatineni, S., Dawson, W.O., 2008. Citrus
912 tristeza virus: survival at the edge of the movement continuum. J. Virol. 82, 6546-
913 6556. doi: 10.1128/JVI.00515-08.

914 Fu, Z.Q., Yan, S., Saleh, A., Wang, W., Ruble, J., Oka, N., Mohan, R., Spoel, S.H.,
915 Tada, Y., Zeng, N., Dong, X., 2012. NPR3 and NPR4 are receptors for the immune
916 signal salicylic acid in plants. Nature 486, 228-232. doi: 10.1038/nature11162.

917 Fuchs, M., Bar-Joseph, M., Candresse, T., Maree, H.J., Martelli, G.P., Melzer,
918 M.J., Menzel, W., Minafra, A., Sabanadzovic, S., 2020. ICTV Virus Taxonomy
919 Profile: *Closteroviridae*. J. Gen. Virol. 101, 364-365. doi: 10.1099/jgv.0.001397.

920 Gandía, M., Conesa, A., Ancillo, G., Gadea, J., Forment, J., Pallás, V., Flores, R.,
921 Duran-Vila, N., Moreno, P., Guerri, J., 2007. Transcriptional response of *Citrus*
922 *aurantifolia* to infection by *Citrus tristeza virus*. Virology 367, 298-306. doi:
923 10.1016/j.virol.2007.05.025.

924 Garcia-Ruiz, H., Takeda, A., Chapman, E.J., Sullivan, C.M., Fahlgren, N.,
925 Brempelis, K.J., Carrington, J.C., 2010. Arabidopsis RNA-dependent RNA
926 polymerases and dicer-like proteins in antiviral defense and small interfering RNA
927 biogenesis during turnip mosaic virus infection. Plant Cell, 22, 481-496. doi:
928 10.1105/tpc.109.073056.

929 Garnsey, S.M., Gonsalves, D., Purcifull, D.E., 1977. Mechanical transmission of
930 citrus tristeza virus. Phytopathology 67, 965-968. doi: 10.1094/Phyto-67-965.

931 Garnsey, S.M., Permar, T.A., Cambra, M., Henderson, C.T., 1993. Direct tissue
932 blot immunoassay (DTBIA) for detection of citrus tristeza virus (CTV), in: Moreno,
933 P., Da Graça, J.V., Timmer, L.W. (Eds.), Proc. 12th Conf. Int. Organ. Citrus Virol.
934 IOCV, Riverside, CA., pp. 39-50.

935 Ghorbel, R., López, C., Fagoaga, C., Moreno, P., Navarro, L., Flores, R., Peña, L.,
936 2001. Transgenic citrus plants expressing the citrus tristeza virus p23 protein
937 exhibit viral-like symptoms. Mol. Plant Pathol. 2, 27-36. doi: 10.1046/j.1364-
938 3703.2001.00047.x.

939 Gollan, P.J., Bhave, M., Aro, E.M., 2012. The FKBP families of higher plants:
940 Exploring the structures and functions of protein interaction specialists. FEBS Lett.
941 586, 3539-3547. doi: 10.1016/j.febslet.2012.09.002.

Gómez-Muñoz, N., Velázquez, K., Vives, M.C., Ruiz-Ruiz, S., Pina, J.A., Flores, R., Moreno, P., Guerri, J., 2017. The resistance of sour orange to *Citrus tristeza virus* is mediated by both the salicylic acid and the RNA silencing defense pathways. Mol. Plant Pathol. 18, 1253-1266. doi: 10.1111/mpp.12488.

Gonsalves, D., Purcifull, D.E., Garnsey S.M., 1978. Purification and serology of citrus tristeza virus. Phytopathology 68, 553-559. doi: 10.1094/Phyto-68-553.

Gottwald, T.R., Cambra, M., Moreno, P., Camarasa, E., Piquer, J., 1996. Spatial and temporal analyses of citrus tristeza virus in Eastern Spain. Phytopathology 86, 45-55. doi: 10.1094/Phyto-86-45

Gottwald, T.R., Garnsey, S.M., Borbón, J., 1998. Increase and patterns of spread of citrus tristeza virus infections in Costa Rica and the Dominican Republic in the presence of the brown citrus aphid, *Toxoptera citricida*. Phytopathology 88, 621-636. doi: 10.1094/PHYTO.1998.88.7.621.

Gowda, S., Satyanayanana, T., Ayllón, M.A., Moreno, P., Flores, R., Dawson, W.O., 2003. The conserved structures of the 5′ non-translated region of *Citrus tristeza virus* are involved in replication and virion assembly. Virology 317, 50-64. doi: 10.1016/j.virol.2003.08.018.

Harper, S.J., 2013. *Citrus tristeza virus*: evolution of complex and varied genotypic groups. Front. Microbio9l. 4, 93. doi: 10.3389/fmicb.2013.00093.

Heinlein, M., 2015. Plant virus replication and movement. Virology 479-480, 657-671. doi: 10.1016/j.virol.2015.01.025.

Hilf, M.E., Karasev, A.V., Pappu, H.R., Gumpf, D.J., Niblett, C.L., Garnsey, S.M., 1995. Characterization of citrus tristeza virus subgenomic RNAs in infected tissue. Virology 208, 576-582. doi: 10.1006/viro.1995.1188.

Jay, F., Wang, Y., Yu, A., Taconnat, L., Pelletier, S., Colot, V., Renou, J.P., Voinnet, O., 2011. Misregulation of *AUXIN RESPONSE FACTOR 8* underlies the developmental abnormalities caused by three distinct viral silencing suppressors in Arabidopsis. PLoS Pathog. 7, e1002035. https://doi.org/10.1371/journal.ppat.1002035

971 Karasev, A.V., Boyko, V.P., Gowda, S., Nikolaeva, O.V., Hilf, M.E., Koonin, E.V.,
972 Niblett, C.L., Cline, K., Gumpf, D.J., Lee, R.F., Garnsey, S.M., Lewandowski, D.J.,
973 Dawson, W.O., 1995. Complete sequence of the citrus tristeza virus RNA genome.
974 Virology, 208, 511-520. doi: 10.1006/viro.1995.1182.

975 Kitajima, E.W., Silva, D.M., Oliveira, A.R., Müller, G.W., Costa, A.S., 1964. Thread-
976 like particles associated with tristeza disease of citrus. Nature 201, 1011-1012.
977 https://doi.org/10.1038/2011011a0.

978 Koonin, E.W., Boyko, V.P., Dolja, V.V., 1991. Small cysteine-rich proteins of
979 different groups of plant RNA viruses are related to different families of nucleic
980 acid-binding proteins. Virology 181, 396-398. doi: 10.1016/0042-6822(91)90512-a.

981 Laird, J., McInally, C., Carr, C., Doddiah, S., Yates, G., Chrysanthou, E., Khattab,
982 A., Love, A.J., Geri, C., Sadanandom, A., Smith, B.O., Kobayashi, K., Milner, J.J.,
983 2013. Identification of the domains of cauliflower mosaic virus protein P6
984 responsible for suppression of RNA silencing and salicylic acid signalling. J. Gen.
985 Virol. 94, 2777-2789. doi: 10.1099/vir.0.057729-0.

986 López, C., Ayllón, M.A., Navas-Castillo, J., Guerri, J., Moreno, P., Flores, R., 1998.
987 Molecular variability of the 5′ and 3′ terminal regions of citrus tristeza virus RNA.
988 Phytopathology 88, 685-691. doi: 10.1094/PHYTO.1998.88.7.685.

989 López, C., Cervera, M., Fagoaga, C., Moreno, P., Navarro, L., Flores, R., Peña, L.,
990 2010. Accumulation of transgene-derived siRNAs is not sufficient for RNAi-
991 mediated protection against *Citrus tristeza virus* in transgenic Mexican lime. Mol.
992 Plant Pathol. 11, 33-41. doi: 10.1111/j.1364-3703.2009.00566.x.

993 López, C., Navas-Castillo, J., Gowda, S., Moreno, P., Flores, R., 2000. The 23-kDa
994 protein coded by the 3′-terminal gene of citrus tristeza virus is an RNA-binding
995 protein. Virology 269, 462-470. doi: 10.1006/viro.2000.0235.

996 Lu, R., Folimonov, A., Shintaku, M., Li, W.X., Falk, B.W., Dawson, W.O., Ding,
997 S.W., 2004. Three distinct suppressors of RNA silencing encoded by a 20-kb viral
998 RNA genome. Proc. Natl. Acad. Sci. U.S.A. 101, 15742-15747. https://doi.org/
999 10.1073/pnas.0404940101.

1000 Mallory, A., Vaucheret, H., 2010. Form, function, and regulation of ARGONAUTE
1001 proteins. Plant Cell 22, 3879-3889. https://doi.org/10.1105/tpc.110.080671.

1002 Martín, S., Sambade, A., Rubio, L., Vives, M.C., Moya, P., Guerri, J., Elena, S.F.,
1003 Moreno, P., 2009. Contribution of recombination and selection to molecular
1004 evolution of *Citrus tristeza virus*. J. Gen. Virol. 90, 1527-1538. doi:
1005 10.1099/vir.0.008193-0.

1006 Mawassi, M., Mietkiewska, E., Gofman, R., Yang, G., Bar-Joseph, M., 1996.
1007 Unusual sequence relationships between two isolates of citrus tristeza virus. J.
1008 Gen.Virol. 77, 2359-2364. doi: 10.1099/0022-1317-77-9-2359.

1009 Medberry, S.L., Lockhart, B.E., Olszewski, N.E., 1992. The commelina yellow
1010 mottle virus promoter is a strong promoter in vascular and reproductive tissues.
1011 Plant Cell 4, 185-192. doi: 10.1105/tpc.4.2.185.

1012 Meneghini, M., 1946. Sobre a naturaleza e transmissibilidade da doença "Tristeza"
1013 dos Citrus. O Biologico 12, 285-287.

1014 Moreno, P., Ambrós, S., Albiach-Martí, M.R., Guerri, J., Peña, L., 2008. *Citrus*
1015 *tristeza virus*: a pathogen that changed the course of the citrus industry. Mol. Plant
1016 Pathol. 9, 251-268. doi: 10.1111/j.1364-3703.2007.00455.x.

1017 Moreno P., Garnsey S.M., 2010. Citrus tristeza diseases - a worldwide perspective,
1018 in: Karasev, A.V., Hilf, M.E. (Eds.), *Citrus tristeza virus* complex and tristeza
1019 diseases. The American Phytopathological Society, St Paul, MN, pp. 27-49.

1020 Navas-Castillo, J., Albiach-Martí, M.R., Gowda, S., Hilf, M.E., Garnsey, S.M.,
1021 Dawson, W.O., 1997. Kinetics of accumulation of citrus tristeza virus RNAs.
1022 Virology 228, 92-97. doi: 10.1006/viro.1996.8369.

1023 Pappu, S.S., Febres, V.J., Pappu, H.R., Lee, R.F., Niblett, C.L., 1997.
1024 Characterization of the 3’ proximal gene of the citrus tristeza closterovirus genome.
1025 Virus Res. 47, 51-57. https://doi.org/10.1016/S0168-1702(96)01405-0.

1026 Pappu, H.R., Karasev, A.V., Anderson, E.J., Pappu, S.S., Hilf, M.E., Febres, V.J.,
1027 Eckloff R.M.G., McCaffery, M., Boyko, V., Gowda, S., Dolja, V.V., Koonin, E.V.,
1028 Gumpf, D.J., Cline, K.C., Garnsey, S.M., Dawson, W.O., Lee, R.F., Niblett, C.L.,

1029 1994. Nucleotide sequence and organization of eight 3' open reading frames of the
1030 citrus tristeza closterovirus genome. Virology 199, 35-46. doi:
1031 10.1006/viro.1994.1095.

1032 Roy, G., Sudarshana, M.R., Ullman, D.E., Ding, S.W., Dandekar, A.M., Falk, B.W.,
1033 2006. Chimeric cDNA sequences from *Citrus tristeza virus* confer RNA silencing-
1034 mediated resistance in transgenic *Nicotiana benthamiana* plants. Phytopathology
1035 96, 819-827. doi: 10.1094/PHYTO-96-0819.

1036 Ruiz-Ruiz, S., Moreno, P., Guerri, J., Ambrós, S., 2006. The complete nucleotide
1037 sequence of a severe stem pitting isolate of *Citrus tristeza virus* from Spain:
1038 comparison with isolates from different origins. Arch. Virol. 151, 387-398. doi:
1039 10.1007/s00705-005-0618-6.

1040 Ruiz-Ruiz, S., Navarro, B., Gisel, A., Peña, L., Navarro, L., Moreno, P., Di Serio,
1041 F., Flores, R., 2011. Citrus tristeza virus infection induces the accumulation of viral
1042 small RNAs (21- 24-nt) mapping preferentially at the 3'-terminal region of the
1043 genomic RNA and affects the host small RNA profile. Plant Mol. Biol. 75, 607-619.
1044 doi: 10.1007/s11103-011-9754-4.

1045 Ruiz-Ruiz, S., Soler, N., Sánchez-Navarro, J., Fagoaga, C., López, C., Navarro, L.,
1046 Moreno, P., Peña, L., Flores, R., 2013. Citrus tristeza virus p23: determinants for
1047 nucleolar localization and their influence on suppression of RNA silencing and
1048 pathogenesis. Mol. Plant-Microbe Interact. 26, 306-318.
1049 https://doi.org/10.1094/MPMI-08-12-0201-R.

1050 Ruiz-Ruiz, S., Spanò, R., Navarro, L., Moreno, P., Peña, L., Flores, R., 2018.
1051 Citrus tristeza virus co-opts glyceraldehyde 3-phosphate dehydrogenase for its
1052 infectious cycle by interacting with the viral-encoded p23 protein. Plant Mol. Biol.
1053 98, 363-373. https://doi.org/10.1007/s11103-018-0783-0.

1054 Sambade, A., López, C., Rubio, L., Flores, R., Guerri, J., Moreno, P., 2003.
1055 Polymorphism of a specific region in the gene *p23* of *Citrus tristeza virus* allows
1056 discrimination between mild and severe isolates. Arch. Virol. 148, 2325-2340. doi:
1057 10.1007/s00705-003-0191-9.

1058 Satyanayanana, T., Bar-Joseph, M., Mawassi, M., Albiach-Martí, M.R., Ayllón,
1059 M.A., Gowda, S., Hilf, M.E., Moreno, P., Garnsey, S.M., Dawson, W.O., 2001.
1060 Amplification of Citrus tristeza virus from a cDNA clone and infection of citrus trees.
1061 Virology, 280, 87-96. doi: 10.1006/viro.2000.0759.

1062 Satyanarayana, T., Gowda, S., Ayllón, M.A., Albiach-Martí, M.R., Rabindram, R.,
1063 Dawson, W.O., 2002. The p23 protein of *Citrus tristeza virus* controls asymmetrical
1064 RNA accumulation. J. Virol. 76, 473-483. doi: 10.1128/JVI.76.2.473-483.2002.

1065 Satyanayanana, T., Gowda, S., Boyko, V.P., Albiach-Martí, M.R., Mawassi, M.,
1066 Navas-Castillo, J., Karasev, A.V., Dolja, V., Hilf, M.E., Lewandowsky, D.J., Moreno,
1067 P., Bar-Joseph, M., Garnsey, S.M., Dawson, W.O., 1999. An engineered
1068 closterovirus RNA replicon and analysis of heterologous terminal sequences for
1069 replication. Proc. Natl. Acad. Sci. U.S.A. 96, 7433-7438. doi:
1070 10.1073/pnas.96.13.7433.

1071 Smith, N.A., Singh, S.P., Wang, M.B., Stoutjesdijk, P.A., Green, A.G., Waterhouse,
1072 P.M., 2000. Total silencing by intron-spliced hairpin RNAs. Nature, 407, 319-320.
1073 doi: 10.1038/35030305.

1074 Soler, N., Fagoaga, C., López, C., Moreno, P., Navarro, L., Flores, R., Peña, L.,
1075 2015. Symptoms induced by transgenic expression of p23 from *Citrus tristeza virus*
1076 in phloem-associated cells of Mexican lime mimics virus infection without the
1077 aberrations accompanying constitutive expression. Mol. Plant Pathol. 16, 388-399.
1078 doi: 10.1111/mpp.12188.

1079 Soler, N., Plomer, M., Fagoaga, C., Moreno, P., Navarro, L., Flores, R., Peña, L.,
1080 2012. Transformation of Mexican lime with an intron-hairpin construct expressing
1081 untranslatable versions of the genes coding for the three silencing suppressors of
1082 Citrus tristeza virus confers complete resistance to the virus. Plant Biotech. J. 10,
1083 597-608. doi: 10.1111/j.1467-7652.2012.00691.x.

1084 Tatineni, S., Dawson, W.O., 2012. Enhancement or attenuation of disease by
1085 deletion of genes from Citrus tristeza virus. J. Virol. 86, 7850-7857. doi:
1086 10.1128/JVI.00916-12.

1087 Tatineni, S., Robertson, C.J., Garnsey, S.M., Dawson, W.O., 2011. A plant virus
1088 evolved by acquiring multiple nonconserved genes to extend its host range. Proc.
1089 Natl. Acad. Sci. U.S.A. 108, 17366-17371. doi: 10.1073/pnas.1113227108.

1090 Vela, C., Cambra, M., Cortés, E., Moreno, P., Miguet, J.G., Pérez de San Román,
1091 C., Sanz, A., 1986. Production and characterization of monoclonal antibodies
1092 specific for citrus tristeza virus and their use for diagnosis. J. Gen. Virol. 67, 91-96.
1093 https://doi.org/10.1099/0022-1317-67-1-91.

1094 Vives, M.C., Rubio, L., López, C., Navas-Castillo, J., Albiach-Martí, M.R., Dawson,
1095 W.O., Guerri, J., Flores, R., Moreno, P., 1999. The complete genome sequence of
1096 the major component of a mild citrus tristeza virus isolate. J. Gen. Virol. 80, 811-
1097 816. doi: 10.1099/0022-1317-80-3-811.

1098 Voinnet, O., Pinto, Y.M., Baulcombe, D.C., 1999. Suppression of gene silencing: A
1099 general strategy used by diverse DNA and RNA viruses of plants. Proc. Natl. Acad.
1100 Sci. U.S.A. 96,14147-14152. doi: 10.1073/pnas.96.24.14147.

1101 Wu, Y., Zhang, D., Chu, J.Y., Boyle, P., Wang, Y., Brindle, I.D., De Luca, V.,
1102 Desproes, C., 2012. The Arabidopsis NPR1 protein is a receptor for the plant
1103 defense hormone salicylic acid. Cell Rep. 1, 639-647. doi:
1104 10.1016/j.celrep.2012.05.008.

1105 Yang, Z.N., Mathews, D.H., Dodds, J.A., Mirkov, T.E., 1999. Molecular
1106 characterization of an isolate of Citrus tristeza virus that causes severe symptoms
1107 in sweet orange. Virus Genes 19, 131-142. doi: 10.1023/a:1008127224147.

1108 Yang, Z., Zhang, Y., Wang, G., Wen, S., Wang, Y., Li, L., Xiao, F., Hong, N., 2021.
1109 The p23 of citrus tristeza virus interacts with host FKBP-type peptidyl-prolylcis-
1110 trans isomerase 17-2 and is involved in the intracellular movement of the viral coat
1111 protein. Cells 10, 934. https://doi.org/10.3390/cells10040934.

1112

FIGURES

Figure 1.- Main diseases caused by CTV (A-C), CTV virions (D) and genome organization (E): A) Tristeza decline incited in sweet orange propagated on sour orange rootstock (left) in comparison with a neighbor tree propagated on a decline-tolerant rootstock, B) Stem pitting induced by a severe CTV isolate in navel sweet orange, C) Seedling yellows produced by a severe strain of CTV in a Duncan grapefruit seedling (right) and non-inoculated control (left), D) Electron micrography of a negatively-stained CTV preparation (28500x magnification) and E) Outline of the CTV genome with the open reading frames (ORFs) indicated by rectangles and the untranslated 5' and 3' terminal regions (5'UTR and 3'UTR) by a dark line. The proteins encoded are indicated in black letters: the two proteases (PRO), methyltransferase (MET), helicase (HEL), RNA-dependent RNA polymerase (RdRp) and the p33, p6, p65, p61, p27, p25, p18, p13, p20 and p23 proteins. The proteins involved in replication, virion assembly and movement, host range, pathogenicity and RNA silencing suppression are indicated by arrows.

Figure 2.- Amino acid sequence and structural features of the p23 protein from the CTV isolate T385 (Spain). The putative zinc-finger motif is outlined, with the cysteine and histidine residues coordinating the Zn ion highlighted with colored background, and the arginine and lysine residues forming part of the domain rich in basic amino acids remarked with bold fonts.

Figure 3.- Distribution by polarity (A and C) and along de CTV genome (B and D) of the CTV-derived small RNAs (sRNAs) produced after infection of a susceptible (Mexican lime) or a partially resistant (sour orange) host. A) and C) represent the polarity (+ or -) distribution of the reads (18-26 nt) perfectly matching the plus (blue) or minus (red) sRNAs. B) and D) represent the density (reads per nt) of the plus and minus sRNA reads (18-26 nt) along the CTV genome (outlined at the top) in each host (From Ruiz-Ruiz et al., 2011).

Figure 4.- Confocal laser scanning microscope images of infection foci taken from the inner side of bark pieces from sour orange (A, C and D) or sweet orange (B) inoculated with a GFP-expressing CTV vector. A) and B) were taken from plants transformed with an empty vector (control) and C) from a p23-transgenic sour orange. D) is a close-up of the area marked in C to show that some foci are formed by several cells (From Fagoaga et al., 2011)

Figure 5.- Leaf symptoms displayed by CTV-infected Mexican lime (A and C) and *Nicotiana benthamiana* (F) plants, and CTV-like symptoms displayed by transgenic limes expressing the *p23* gene of CTV under the control of the 35S promoter of CaMV (B, D and E). A) and C) Non-transgenic limes infected with the CTV isolates T36 (A) and T317 (C), respectively. B) and D) Transgenic limes expressing the p23 protein from T36 and T317, respectively. E) Lime transformed with a truncated version of the T36-*p23* gene. F) *N. benthamiana* agroinoculated with an infectious cDNA clone of T36 (right) and a CTV-free control (left). (Pictures A-E from Fagoaga et al., 2005).

1161 Fig. 1.

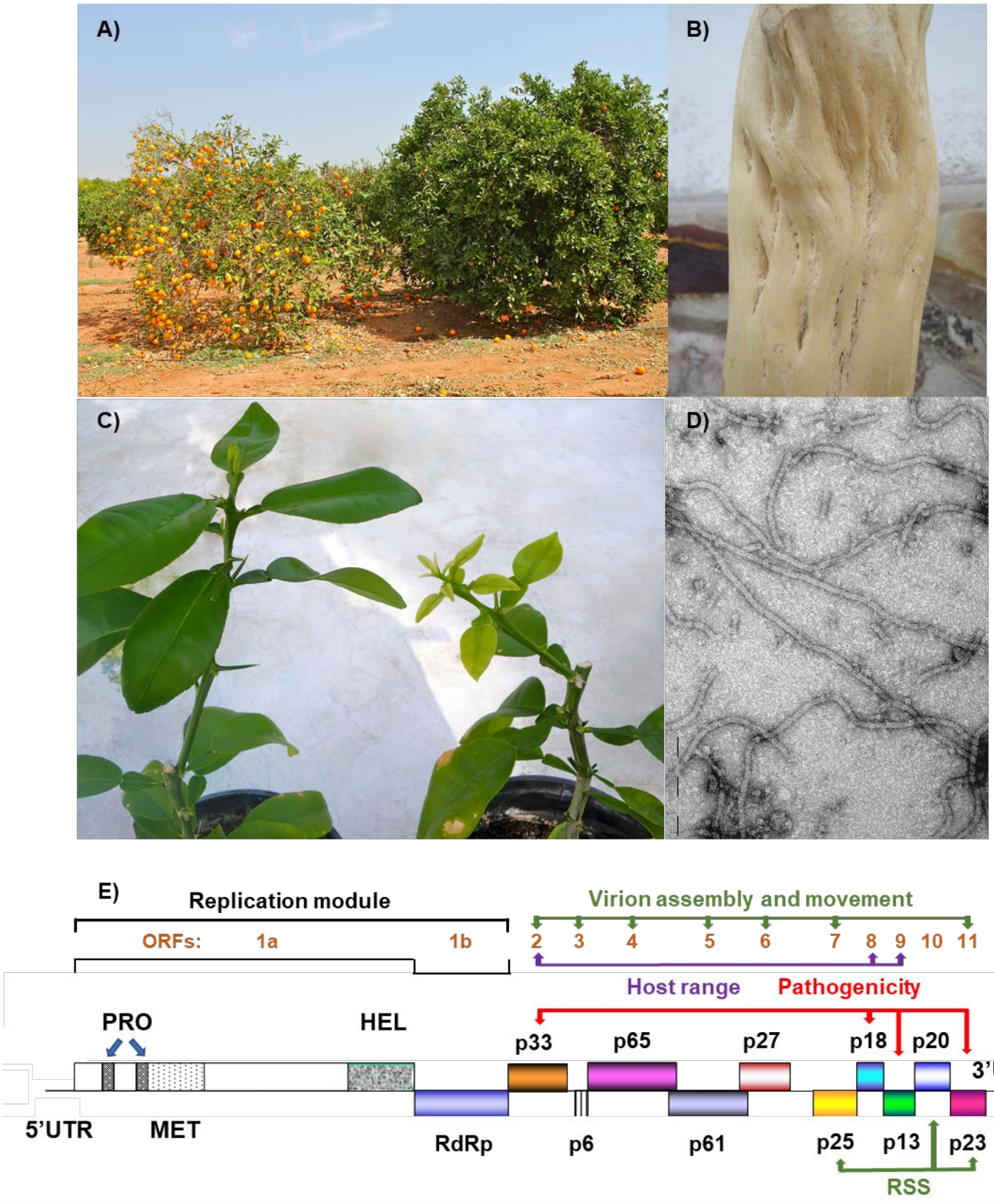

1162

Fig. 2.

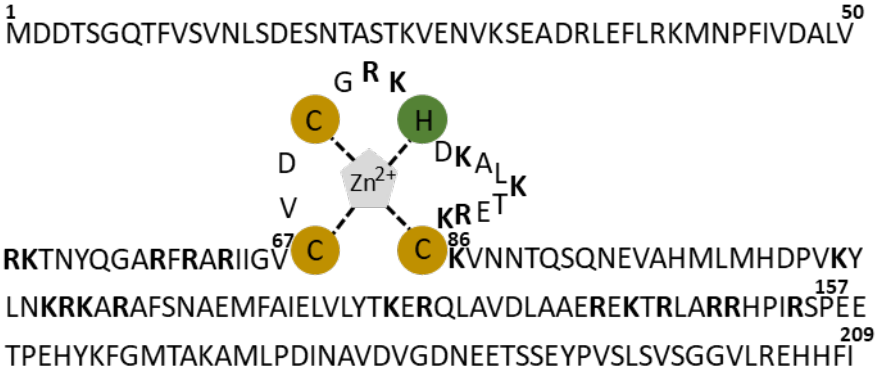
1
MDDTSGQTFVSVNLSDESNTASTKVENVKSEADRLEFLRKMNPFIVDALV
50
G R K
C
H
D
D K A L K
Zn2+
V
K R E T
67 C
C 86
RKTNYQGARFRARIIGV
KVNNTQSQNEVAHMLMHDPVKY
LNKRKARAFSNAEMFAIELVLYTKERQLAVDLAAEREKTRLARRHPIRSPEE
157
TPEHYKFGMTAKAMLPDINAVDVGDNEETSSEYPVSLSVSGGVLREHHFI
209

Fig. 3.

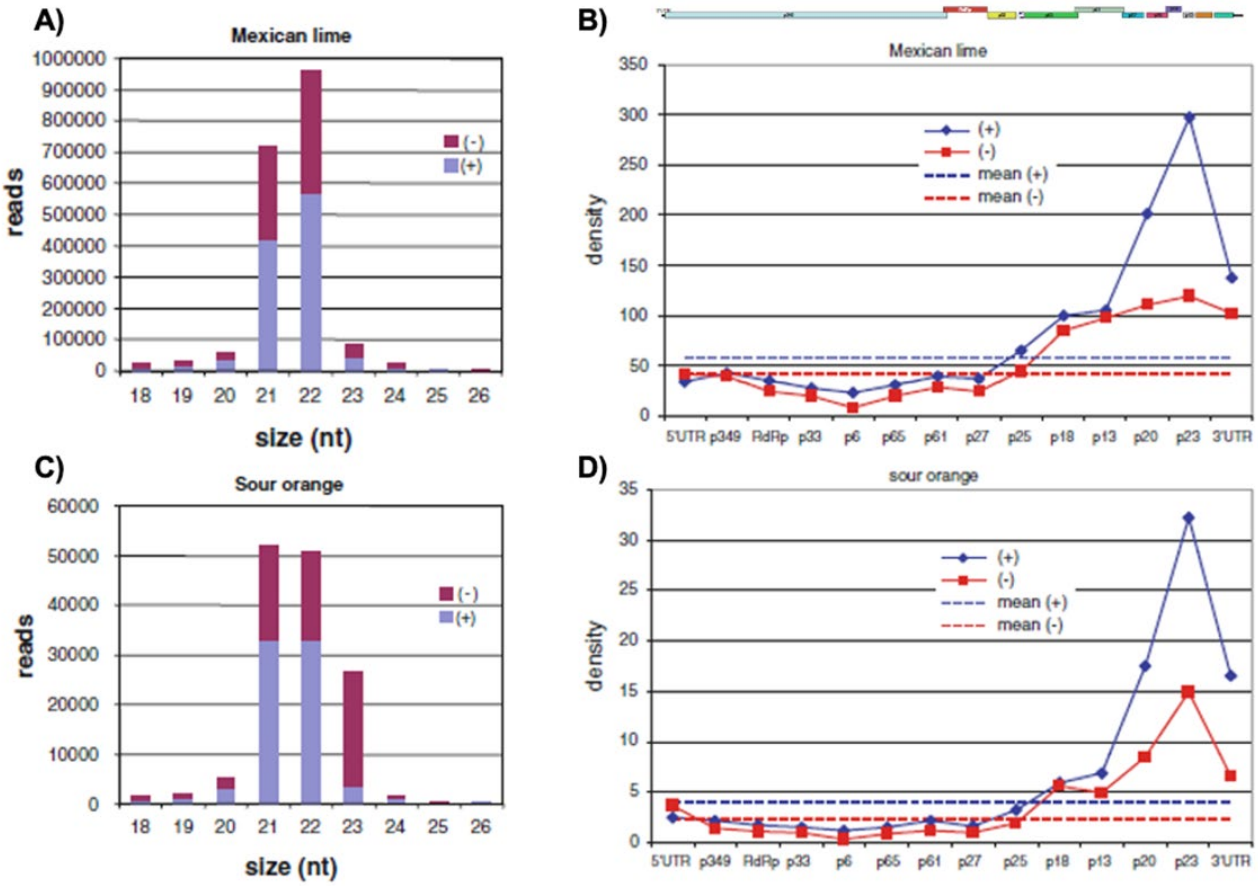
A)
Mexican lime
reads
size (nt)
(-)
(+)
B)
Mexican lime
density
mean (+)
mean (-)
5'UTR p349 RdRp p33 p6 p65 p61 p27 p25 p18 p13 p20 p23 3'UTR
C)
Sour orange
reads
size (nt)
D)
sour orange
density

1172 Fig. 4.

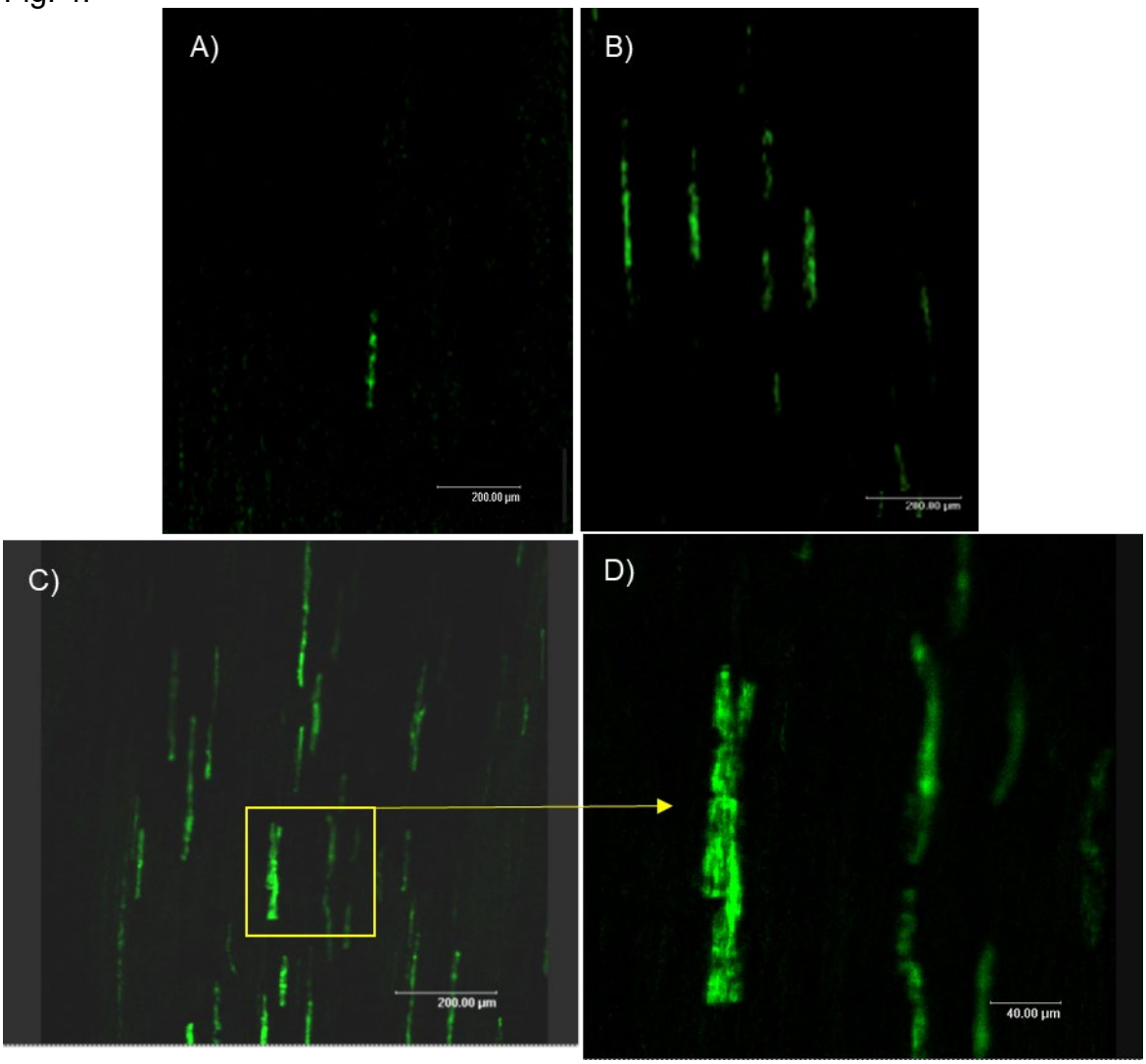

1173
1174
1175

1176 Fig. 5.

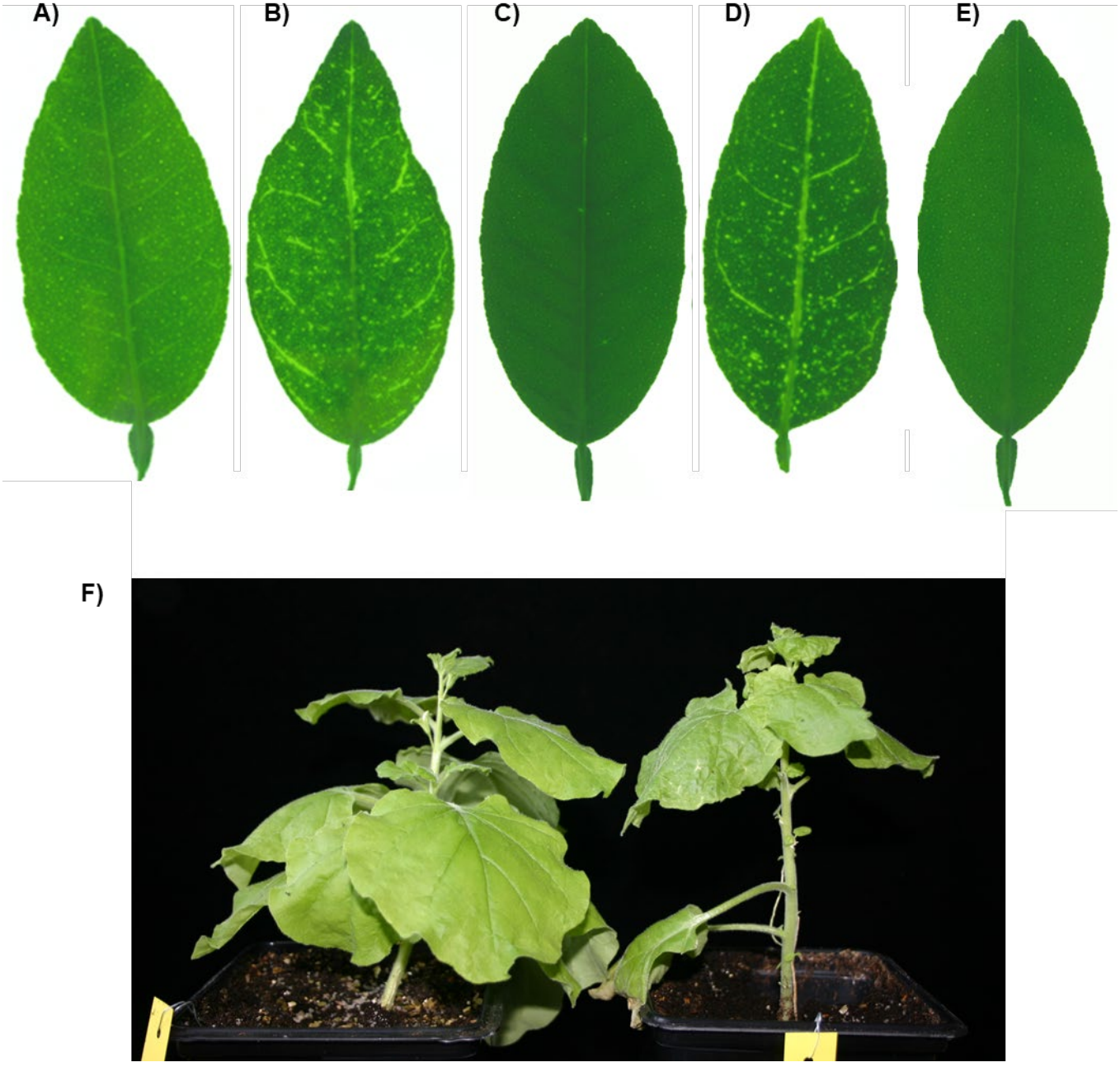

1177